

The CZCS data demonstrate that phytoplankton in the western Ross Sea can bloom early, with great intensity, and persist for a long time under conditions that produce and sustain the Ross Sea polynya. Estimates of annual productivity in the western Ross Sea should be revised upward; hence, the relative importance of this region as a CO₂ sink may be greater than previously recognized. It is unfortunate that the CZCS did not provide imagery of the 1978–79 spring phytoplankton bloom earlier than 10 December so that early bloom dynamics could have been monitored. Future satellite ocean color missions, such as the sea-viewing wide field-of-view sensor (SeaWiFS) and the moderate-resolution imaging spectrometer (MODIS), should alleviate this problem by providing data at much finer temporal resolution.

REFERENCES AND NOTES

1. S. Z. El-Sayed *et al.*, *Deep-Sea Res.* **30**, 871 (1983).
2. D. C. Biggs *et al.*, in *Antarctic Nutrient Cycles and Food Webs*, W. R. Siegfried *et al.*, Eds. (Springer-Verlag, Berlin, 1985), pp. 93–103.
3. D. C. Biggs *et al.*, *Tex. A&M Univ. Org. Res. 85-6-T* (Department of Oceanography, Texas A&M University, College Station, 1985).
4. D. L. Wilson *et al.*, *Deep-Sea Res.* **33**, 1375 (1986).
5. W. O. Smith Jr., *et al.*, *Antarct. J. U.S.* **25**, 179 (1990).
6. D. J. Demaster *et al.*, *Oceanography* **5**, 146 (1992).
7. J. C. Comiso and C. W. Sullivan, *J. Geophys. Res.* **91**, 9663 (1986).
8. C. W. Sullivan, K. R. Arrigo, C. R. McClain, J. C. Comiso, J. Firestone, *Science* **262**, 1832 (1993).
9. A. C. Palmisano *et al.*, *J. Plankton Res.* **8**, 891 (1986).
10. J. P. Barry, *Polar Biol.* **8**, 377 (1988).
11. ——— and P. K. Dayton, *ibid.*, p. 367.
12. R. W. Eppley *et al.*, *J. Plankton Res.* **7**, 57 (1985).
13. O. Holm-Hansen *et al.*, in *Adaptations Within Antarctic Ecosystems*, G. A. Llano, Ed. (Smithsonian Institution, Washington DC, 1977), pp. 11–50.
14. W. O. Smith Jr. and D. M. Nelson, *Limnol. Oceanogr.* **35**, 809 (1990).
15. ———, *BioScience* **26**, 251 (1986).
16. C. R. McClain *et al.*, *NASA TM 100728* [National Aeronautics and Space Administration (NASA) Goddard Space Flight Center, Greenbelt, MD, 1991].
17. K. R. Arrigo and C. R. McClain, *NASA TM 104566* (NASA Goddard Space Flight Center, Greenbelt, MD, 1994), vol. 32.
18. J. L. Mueller, *Appl. Opt.* **27**, 438 (1988).
19. H. R. Gordon *et al.*, *ibid.* **22**, 20 (1983).
20. B. G. Mitchell and O. Holm-Hansen, *Deep-Sea Res.* **38**, 1009 (1991).
21. We thank B. Schieber and G. Fu for assistance with image processing, O. Holm-Hansen and D. Biggs for helpful discussions and advice, and M. Lizotte, C. Brown, and L. Harding for editorial comments. Supported by NASA grants 5024 and RTOP 579-11-01-01.

11 April 1994; accepted 14 July 1994

Coupled Land-Ocean-Atmosphere Processes and South Asian Monsoon Variability

Gerald A. Meehl

Results from a global coupled ocean-atmosphere climate model and a model with specified tropical convective heating anomalies show that the South Asian monsoon was an active part of the tropical biennial oscillation (TBO). Convective heating anomalies over Africa and the western Pacific Ocean associated with the TBO altered the simulated pattern of atmospheric circulation for the Northern Hemisphere winter mid-latitude over Asia. This alteration in the mid-latitude circulation maintained temperature anomalies over South Asia through winter and helped set up the land-sea temperature contrast for subsequent monsoon development. South Asian snow cover contributed to monsoon strength but was symptomatic of the larger scale alteration in the mid-latitude atmospheric circulation pattern.

Coupled climate interactions between the ocean and atmosphere contribute to a mechanism that produces biennial variability (TBO) in the troposphere and upper ocean in the tropical Indian and Pacific ocean regions (1, 2). The notion of such coupling has been central to studies of tropospheric biennial oscillations (3), and several researchers have linked the biennial component of variability to El Niño–Southern Oscillation (ENSO) (4–7). The TBO is associated with modulations of the seasonal cycle, with maxima in the TBO manifested as warm (El Niño) and cold (La Niña) ex-

tremes in the tropical Pacific, modulations that have connections to the Indian monsoon (1). A biennial component of tropospheric variability is seen in the tropical Pacific and Indian regions in sea-surface temperature (SST) and surface wind (8–12), and in the western Pacific, in ocean dynamics (13–15). A possible association between the stratospheric quasi-biennial oscillation (QBO) of zonal wind and interannual variability in the tropical troposphere has also been suggested (16, 17). The focus of this report is the extent to which the South Asian monsoon is involved as an active or passive participant in the TBO (and, by extension, ENSO) and the mechanisms by which this interaction occurs.

The land-sea temperature contrast is the basic forcing of the South Asian monsoon (of which the Indian monsoon is an integral part) (18). More accurately, there is a meridional temperature gradient extending from the tropical Indian Ocean north to the Asian land mass that develops through a considerable depth of the troposphere because South Asia heats more quickly than does the Indian Ocean in spring. Heated air over land rises and draws moist, low-level maritime air inland, where convection and heavy precipitation occur during northern summer to fuel the monsoon circulation further. Such land-sea temperature contrasts are important in other tropical rainfall regimes (19) as well as for the simulation of monsoon rainfall in various general circulation models (GCMs) (20) and in paleoclimate studies (21). Consequently, the South Asian monsoon could be actively involved in the TBO and ENSO through modulations of temperature contrast between South Asian land areas and the Indian Ocean.

Links between the South Asian monsoon and the Southern Oscillation have also been shown to have a biennial tendency (22–25). Additionally, snow cover may alter land-surface temperature and subsequent monsoon strength, as suggested in the late 1800s (26). Years with enhanced winter and spring snow cover over South Asia tend to have below-normal monsoon rainfall (27–30). Consequently, tropical–mid-latitude interaction has also been proposed as playing some role in monsoon evolution (24).

The National Center for Atmospheric Research's (NCAR's) coarse-grid, global coupled ocean-atmosphere GCM (31) was used to study the processes postulated above. This type of model is a useful tool for elucidating basic processes in the coupled climate system. It can represent aspects of the observed large-scale mean climate (31), climate variability compared to satellite observations (32), and some elements of ENSO-related variability (33). Because there are no correction terms used to force the coupled model to the observed state, the model-simulated SSTs in the tropics tend to be too cool, thus enhancing land-sea temperature contrast in the monsoon region. Yet, the pattern of mean monsoon seasonal precipitation and the variability of the simulated South Asian monsoon has been shown to be comparable to the observed pattern (34).

The atmospheric model had an approximate horizontal resolution of 4.5° latitude and 7.5° longitude with nine vertical levels. Soil moisture was parameterized by a simple reservoir formulation, and clouds, precipitation, snowfall, and resulting snow cover were computed. The global dynamical ocean model had a resolution of 5° by 5°

National Center for Atmospheric Research, Post Office Box 3000, Boulder, CO 80307–3000, USA.

with four vertical layers and accounted for sea ice with a simple thermodynamic formulation. An integration was performed, without flux correction for present-day climate, for 70 years, the last 50 years of which are analyzed here.

I composited area averages from the coupled model on the basis of an area-averaged index of Indian monsoon rainfall that was the average of all land points over the Indian region for the 50-year time series for the June, July, and August (JJA) season. Using extreme wet or dry seasons (in excess of 1 standard deviation), I computed area averages for various other parameters. Differences were formulated as a function of season for strong-minus-weak monsoons (Fig. 1), with the sign of those differences indicative of a strong monsoon. Maximum magnitudes of these differences were about 5 to 20% of the strong or weak monsoon averages and in most cases were around 1 standard deviation of the monsoon seasonal values.

The coupled model produced a number of similarities to the observed results (Fig. 1). In particular, South Asian land temperatures were elevated (in relation to Indian Ocean SSTs) in the northern winter and spring before a strong monsoon to produce an enhanced land-sea temperature contrast. This contrast was associated with reduced Asian snow cover. During JJA of a strong monsoon (JJA₀), the South Asian land temperatures decreased as soil moisture amounts increased because of heavy rainfall. The cool South Asian land temperatures persisted through the following northern fall, winter, and spring seasons to con-

tribute to decreased land-sea temperature contrast and a relatively weak monsoon the following JJA (JJA₊₁). The cool South Asian land temperatures were associated with increased South Asian snow cover during northern winter [December, January, and February (DJF₊₁)] and spring [March, April, and May (MAM₊₁)].

For the ocean-atmosphere biennial mechanism described earlier, upper-ocean heat-content anomalies provided the "memory" for the 1-year time scale of SST anomalies (2). The land surface does not possess such heat storage characteristics, but soil moisture could provide some memory because it is an accumulated quantity. In the coupled model, elevated soil moisture levels that occurred in conjunction with the strong monsoon in JJA₀ persisted into northern fall [September, October, and November (SON₀)] (Fig. 1). The wetter land surface was associated with enhanced evaporation and cooler land temperatures. By the following northern winter, the soil moisture differences were near zero. Additionally, those differences were also near zero before a strong monsoon during DJF₀ and MAM₀. Surface hydrology appears to have contributed to land-surface temperature anomalies for only part of the year. Consequently, other processes must have been at work to maintain South Asian land-surface temperature anomalies on the 1-year time scale.

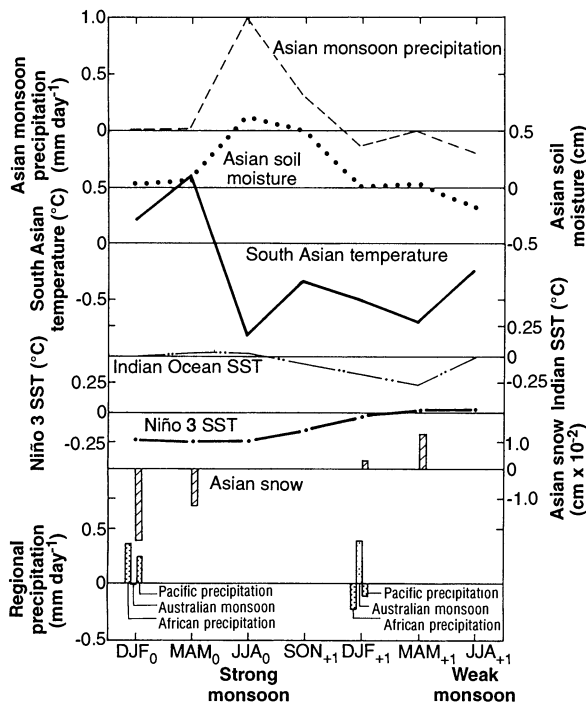
Tropical convective heating anomalies are thought to force anomalous mid-latitude circulation by inducing a remote Rossby wave response (35, 36). Such forcing could affect mid-latitude circulation

that in turn affects the monsoon (24). Studies have shown connections between the tropics and mid-latitudes that affect the South Asian monsoon as well (37). Perhaps heating from anomalous convection associated with the coupled air-sea biennial mechanism that operates in the tropical Indian and Pacific ocean regions (1, 2) could be altering the mid-latitude circulation so as to contribute to the persistence of the surface temperature anomalies over South Asia and thus to monsoon development.

To investigate this hypothesis, I calculated surface temperature anomalies from the coupled model for the DJF season before a strong monsoon (DJF₀, Fig. 2A). Positive differences were located over much of South Asia (as noted by the W's in Fig. 1). Magnitudes of these differences were in excess of 0.5°C in areas of South Asia and up to around 3°C over North Asia. Interannual standard deviations of northern winter surface temperatures from the 50-year integration were 0.8° to 1.0°C over South Asia and were near 2.5°C over North Asia. The 500-mbar height differences (standard deviations averaged about 10 to 15 m over South Asia and near 20 to 25 m over North Asia) showed a well-organized large-scale pattern. Negative differences of about 10 m were located over the Middle East, with positive differences of greater than 35 m over North Asia and negative differences of about 15 m over Northeast Asia (Fig. 2B). This pattern indicates an alteration of the mid-latitude atmospheric circulation such that there was an anomalous ridge of high pressure over Asia (H in Fig. 2B). Such a pattern would help maintain relatively warm surface temperatures over South Asia as a result of southerly advection of warm air under the ridge (38). A further indication that warm air was advected over South Asia in the coupled model is that the sensible heat flux over that region was +7 W m⁻² (the positive sign indicates that warm surface air heated the ground), or about 10% of the mean value for that time of year.

To investigate whether similar patterns were present in observations, I then computed observed differences in surface temperature represented by the European Centre for Medium-Range Weather Forecasts (ECMWF) analyses (39) for the northern winter 1988 (that is, December 1987 and January and February 1988) minus those for northern winter 1987 (Fig. 2C). The 1988 monsoon season was strong, and the 1987 season was weak (40, 41). Therefore, these differences have the sign of conditions that precede a strong monsoon. Similar to but larger than the coupled model composites, positive surface temperature differences of several degrees occurred over most of South Asia and North Asia and negative differ-

Fig. 1. Biennial sequence formed as differences of strong-minus-weak Asian monsoon seasonal composites relative to the strong monsoon season noted JJA₀ from the global coupled climate model. Areas are defined as follows, beginning with the Asian monsoon precipitation and soil moisture: land points, 5°N to 40°N, 60°E to 100°E; South Asian land temperatures: 2°N to 30°N, 70°E to 120°E; Asian snow: liquid water equivalent, 20°N to 70°N, 50°E to 130°E; Indian SST: 5°S to 30°N, 50°E to 100°E; Australian monsoon precipitation: all points, 25°S to equator, 100°E to 150°E; African precipitation: land points, 5°N to 5°S, 15°E to 35°E; Pacific precipitation: all points, 0° to 15°N, 150°E to 170°E; Niño 3 SST: 10°S to 10°N, 150°W to 90°W.



ences occurred over Central Asia (Fig. 2C). Also similar to the coupled model values but with increased amplitude, negative 500-mbar height differences of near 30 m (Fig. 2D) were located over the Middle East, positive differences of over 100 m occurred over North Asia, and negative differences of about 40 m were present over East Asia. This pattern signifies the presence of an anomalous ridge of high pressure over Asia in the winter before the strong monsoon year (1988) compared to the pressure during the winter before the weak monsoon year (1987). The smaller amplitude anomaly patterns in the coupled model (Fig. 2, A and B) compared to the observed values (Fig. 2, C and D) were typical of the lower amplitude tropical variability in the model (33, 34). However, the patterns were similar enough to justify proceeding with an additional sensitivity experiment to test the hypothesis that anomalous heat sources associated with tropical convective heating anomalies could be altering the mid-latitude circulation (and consequent surface temperature anomalies) by remote Rossby wave response.

An atmospheric GCM similar to the one used in the coupled model was run in perpetual January mode with specified climatological SSTs and fixed surface wetness and snow cover. In this model, anomalous convective heat sources and sinks were specified in a manner similar to that in a previous experiment (42). The sources and sinks corresponded to tropical precipitation anomalies suggested by the observations (1, 8, 22) and the coupled model (Fig. 1). The heat sources were centered at 30°E at the equator over continental Africa and at 160°E at the equator over the Pacific. A heat sink was placed at 130°E at the equator over Australasia. Area averages of observed outgoing long-wave radiation (OLR, a proxy for precipitation) were calculated for similar areas to form the 1988 minus 1987 differences and showed rough correspondence to the specified heating anomalies in those regions.

Surface temperature differences from the specified heating experiment (Fig. 2E) showed warming greater than 2°C over South Asia and more than 5°C over North Asia, with standard deviations similar to those in the coupled model. This pattern is in rough agreement with the coupled model and the observations (Fig. 2, A and C). The associated 500-mbar height difference map (Fig. 2F) showed a similar pattern: Negative differences were about 40 m over the Middle East, positive values exceeded 60 m over North Asia, and negative values were over East Asia and the Northwest Pacific. These anomalies were larger than those noted for the coupled model and approached those seen in the observations (Fig. 2, B and D).

This result suggests that tropical-mid-latitude interaction was probably qualitatively correct in the coupled model but that the amplitudes were too low, as is typical of that model (32, 33).

The results from this sensitivity experiment indicate that anomalous heating from convective anomalies related to the coupled atmosphere-ocean biennial mechanism, and associated alteration of the large-scale east-west atmospheric circulation in the tropics with connections to African precipitation (22), could produce changes in the mid-latitude circulation. Consequently, South Asian land-surface temperature anomalies could be maintained by anomalous heat transport caused by such

shifts in the mid-latitude atmospheric circulation patterns.

To examine this possibility further, I computed surface temperature differences for the northern winter season after a strong monsoon and before a weak monsoon (DJF₊₁ in the convention of Fig. 1) for the coupled model. Additionally, I calculated the DJF differences for 1989 minus 1988, representing the period after the strong 1988 monsoon, from the observations. I also performed the corresponding calculation for the specified heating experiment by specifying negative heating anomalies (representative of suppressed convection and, thus, of a heating deficit) centered at 30°E at the equator and 160°E at the equator as

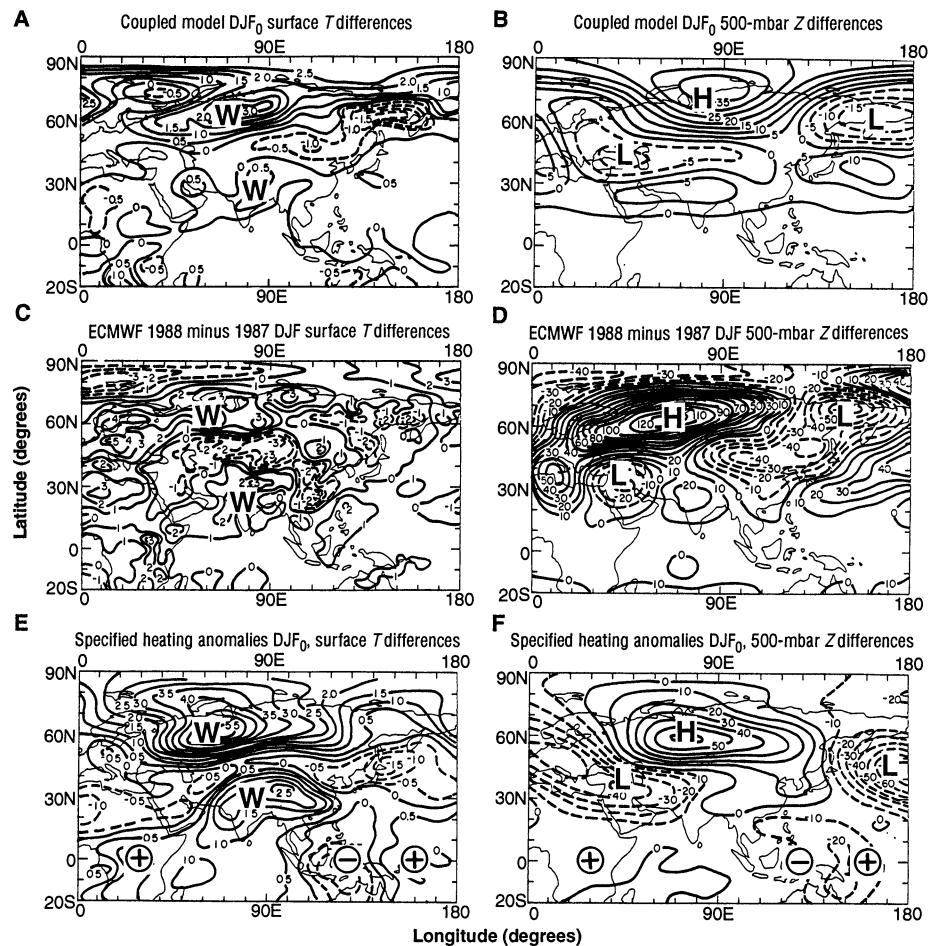


Fig. 2. (A) Surface temperature anomalies with signs representative of DJF₀ before a strong monsoon (Fig. 1) for the coupled model formed from strong-minus-weak monsoon composites. Positive contours are solid, and negative contours are dashed. (B) Same as (A) except for 500-mbar height anomalies. (C) Same as (A) except for observed surface temperature differences, DJF 1988 minus 1987. (D) Same as (C) except for 500-mbar height anomalies. (E) Same as (A) except for specified heating anomaly model of perpetual January with anomalous convective heat sources at the equator, at 30°E, and at the equator 160°E and with anomalous cooling located at the equator 130°E. (F) Same as (E) except for 500-mbar height anomalies. Major warm surface temperature areas in (A), (C), and (E) are denoted by W. Key negative or anomalously low 500-mbar height centers are marked with L, whereas major positive or anomalously high 500-mbar height centers are labeled with an H. The anomalous convective heating (designated by +) or cooling (-) in (E) and (F) was sinusoidal in the vertical with a mid-tropospheric maximum of 5°C and decreased linearly away from the central point in all directions to a radius of 1500 km. Differences were formed by taking a 795-day average, days 100 to 895, from the experiment minus a 2700-day average, days 100 to 2800, from a control integration.

well as a positive heating anomaly placed over Australasia and centered at 130°E at the equator. All showed patterns nearly opposite to those seen in the northern winter before a strong monsoon (Fig. 2). The analogous area-averaged differences of coupled model precipitation corresponded to these specified heating anomalies (Fig. 1). Observed OLR differences showed a comparable combination of apparent heating and cooling over these regions as well.

I suggest that a combination of tropical-mid-latitude forcings associated with tropical SST anomalies during northern winter caused the land-sea (or meridional tropospheric) temperature contrast for the subsequent monsoon (Fig. 3, A and B). Tropical biennial air-sea coupling, consequent SST anomalies, and atmospheric east-west (Walker-type) circulations on the large-scale influence the convective precipitation and associated tropospheric heating anomalies, which then reverse these precipitation and heating trends the following northern winter. The resulting cooler South Asian land temperatures and increased snow cover produce a decreased land-sea temperature contrast and a weak monsoon the following northern summer (Fig. 3, C and D).

A number of other sensitivity experiments were carried out with anomalous equatorial convective heating and cooling centers shifted to various longitudes to represent other features in the empirical orthogonal functions of observed and model-simulated precipitation. Only combinations involving heating and cooling anomalies

over the Pacific, Australasia, and Africa produced the appropriate mid-latitude response over Asia. These results indicate that African precipitation anomalies and associated convective heating anomalies, acting in concert with convective heating anomalies over the western Pacific, could contribute to mid-latitude conditions conducive to subsequent Indian monsoon development. For this sequence of connections, the South Asian monsoon is an active participant in TBO (and, by extension, in ENSO).

In the coupled model (Fig. 1), Asian snow cover was connected to the Asian monsoon. There was less snow in the winter and spring before a strong monsoon and more snow before a weak monsoon. However, the specified heating experiments showed that tropical convective heating anomalies altered the atmospheric circulation pattern over Asia. These changes provided anomalously warm or cold land-surface conditions that could contribute to land-sea temperature contrast without any feedbacks from snow cover (snow areas and surface moisture were specified and could not change in that model). The results from the coupled model suggest that Asian snow cover anomalies contributed positively to the land temperature anomalies. However, the changes of snow cover appear to be an artifact of the shift of the mid-latitude circulation pattern forced by convective heating anomalies. These changes were associated with dynamic air-sea coupling and alteration of the large-scale east-west circula-

tion in the tropics influenced by precipitation anomalies over Africa and the western Pacific.

These results need to be examined further in the context of an improved global coupled GCM that better resolves ENSO processes and in a model with a tropical convective scheme that could better simulate the magnitude of convective heating anomalies. Further observational studies are also required to document these relations with a longer time series. However, the processes outlined here involving the TBO, ENSO, and tropical-mid-latitude interaction provide a framework for understanding variability of the dynamically coupled climate system that connects different regions of the planet.

REFERENCES AND NOTES

- G. A. Meehl, *Mon. Weather Rev.* **115**, 27 (1987).
- , *J. Clim.* **6**, 31 (1993).
- G. W. Brier, *Mon. Weather Rev.* **106**, 938 (1978).
- K. E. Trenberth, *Q. J. R. Meteorol. Soc.* **101**, 55 (1975).
- N. Nicholls, *Mon. Weather Rev.* **106**, 1505 (1978).
- , *Q. J. R. Meteorol. Soc.* **105**, 93 (1979).
- , *Mon. Weather Rev.* **112**, 424 (1984).
- K.-M. Lau and P. J. Sheu, *J. Geophys. Res.* **93**, 10975 (1988).
- E. M. Rasmusson, X. Wang, C. F. Ropelewski, *J. Mar. Syst.* **1**, 71 (1990).
- T. P. Barnett, *J. Clim.* **4**, 269 (1991).
- K. Kutsuwada, *J. Meteorol. Soc. Jpn.* **69**, 687 (1991).
- C. F. Ropelewski, M. S. Halpert, X. Wang, *J. Clim.* **5**, 594 (1992).
- R. Lukas, *J. Geophys. Res.* **93**, 6744 (1988).
- T. Yasunari, *Meteorol. Atmos. Phys.* **44**, 29 (1990).
- Y. Masumoto and T. Yamagata, *J. Phys. Oceanogr.* **21**, 1386 (1991).
- T. Yasunari, *J. Meteorol. Soc. Jpn.* **67**, 483 (1989).
- W. M. Gray, J. D. Sheaffer, J. A. Knaff, *ibid.* **70**, 975 (1992).
- P. J. Webster, in *Monsoons*, J. S. Fein and P. L. Stephens, Eds. (Wiley, New York, 1987), pp. 3–32.
- J. Charney, W. J. Quirk, S.-H. Chow, J. Kornfeld, *J. Atmos. Sci.* **34**, 1366 (1977).
- G. A. Meehl, *J. Clim.* **7**, 1033 (1994).
- J. E. Kutzbach, W. L. Prell, W. F. Ruddiman, *J. Geol.* **101**, 177 (1993).
- G. N. Kiladis and H. van Loon, *Mon. Weather Rev.* **116**, 120 (1988).
- P. J. Webster and S. Yang, *Q. J. R. Meteorol. Soc.* **118**, 877 (1992).
- T. Yasunari and Y. Seki, *J. Meteorol. Soc. Jpn.* **70**, 177 (1992).
- E. M. Rasmusson and T. H. Carpenter, *Mon. Weather Rev.* **111**, 517 (1983).
- H. F. Blanford, *Proc. R. Soc. London* **37**, 3 (1884).
- D. J. Hahn and J. Shukla, *J. Atmos. Sci.* **33**, 2461 (1976).
- J. Shukla, in (18), pp. 399–464.
- T. P. Barnett, L. Dümenil, U. Schlese, E. Roeckner, M. Latif, *J. Atmos. Sci.* **46**, 661 (1989).
- T. Yasunari, A. Kitoh, T. Tokioka, *J. Meteorol. Soc. Jpn.* **69**, 473 (1991).
- W. M. Washington and G. A. Meehl, *Clim. Dyn.* **4**, 1 (1989).
- G. A. Meehl, M. Wheeler, W. M. Washington, *ibid.*, in press.
- G. A. Meehl, *J. Clim.* **3**, 72 (1990).
- and W. M. Washington, *Science* **260**, 1101 (1993).
- G. W. Branstator, *J. Atmos. Sci.* **40**, 1689 (1983).
- , *Proceedings of the TOGA International Scientific Conference*, Honolulu, HI, 16 to 20 July 1990 (World Meteorological Organization, Geneva, 1990).

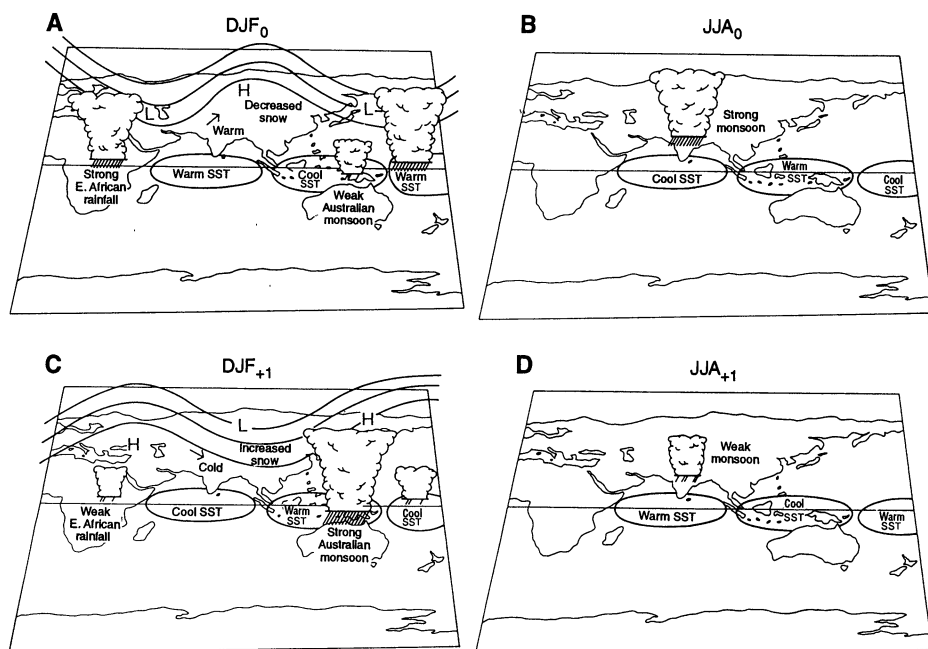


Fig. 3. Schematic biennial evolution from the northern winter before a strong Asian monsoon (A) through the strong monsoon season (B), to the northern winter after the strong monsoon before a weak monsoon (C), to the following weak monsoon (D).

37. T. P. Barnett, *J. Clim.* **1**, 225 (1988).
 38. H. van Loon and J. Williams, *Mon. Weather Rev.* **105**, 636 (1977).
 39. K. E. Trenberth, *NCAR Tech. Note NCAR/TN-373+STR* (NCAR, Boulder, CO, 1992).
 40. T. N. Krishnamurti, H. S. Bedi, M. Subramanian, *J. Clim.* **2**, 321 (1989).
 41. ———, *Meteorol. Atmos. Phys.* **42**, 19 (1990).
 42. G. A. Meehl, G. W. Branstator, W. M. Washington, *J. Clim.* **6**, 42 (1993).

43. I thank G. Branstator and A. Mai for collaboration on the specified heating experiments. A portion of this study was supported by the Office of Health and Environmental Research, U.S. Department of Energy, as part of its Carbon Dioxide Research Program. The National Center for Atmospheric Research is sponsored by the National Science Foundation.

28 June 1994; accepted 29 August 1994

Early Cretaceous Dinosaurs from the Sahara

Paul C. Sereno*, Jeffrey A. Wilson, Hans C. E. Larsson, Didier B. Dutheil, Hans-Dieter Sues

A major question in Mesozoic biogeography is how the land-based dinosaurian radiation responded to fragmentation of Pangaea. A rich fossil record has been uncovered on northern continents that spans the Cretaceous, when continental isolation reached its peak. In contrast, dinosaur remains on southern continents are scarce. The discovery of dinosaurian skeletons from Lower Cretaceous beds in the southern Sahara shows that several lineages of tetanuran theropods and broad-toothed sauropods had a cosmopolitan distribution across Pangaea before the onset of continental fragmentation. The distinct dinosaurian faunas of Africa, South America, and Asiamerica arose during the Cretaceous by differential survival of once widespread lineages on land masses that were becoming increasingly isolated from one another.

Although increased continental isolation has been implicated as the driving force behind the differentiation of Cretaceous dinosaurian faunas (1), a coherent picture of dinosaurian biogeography during this period has not been possible because of the near absence of fossil evidence from key southern land masses such as Africa. With rare exceptions (2, 3), available information on Cretaceous dinosaurs from Africa is based on preliminary paleontological surveys in the Sahara (4), isolated or fragmentary bones and teeth (5), and a small fossil collection from Egypt that was destroyed during World War II (6, 7). We report here on the discovery of dinosaurs from Lower Cretaceous rocks in the southern Sahara Desert (Fig. 1) that impact on the understanding of late Mesozoic dinosaurian biogeography.

The fossils include the first relatively complete skeleton of a theropod dinosaur from the Cretaceous of Africa, *Afrovenator abakensis*, n. gen. n. sp. (8). The skull is low compared to that of other large-skulled predators such as *Allosaurus* (9). Maximum height at the orbit is less than one-third the skull length (Fig. 2A). Unlike *Allosaurus* and many other theropods, cranial crests and rugosities are poorly developed. The

lacrimal crest, for example, has a low, rounded profile. As in many theropods, the lacrimal crest is hollowed by a pneumatic cavity. The maxilla has a slit-shaped premaxillary fenestra, a small, posteriorly positioned maxillary fenestra, and sockets for 14 blade-shaped teeth. The quadrate is tall with a dorsoventral length more than one-half the skull height at the orbit.

The skeleton is relatively gracile judging from the length and diameter of the long bones (Fig. 2C). Cervical vertebrae have deep pleurocoel cavities and articulate in an upward curve that elevates the skull above the dorsal column. The forelimb appears to be similar in length to that of *Allosaurus* but has different proportions within the limb.



Fig. 1. Paleogeographic map of land surfaces during the Early Cretaceous (Barremian-Hauterivian, 130 million years ago). Mollweide projection with latitude and longitude lines spaced at 30° intervals (longitude greater than 120° not shown) (37). +, dinosaur locality.

In *Afrovenator* the humerus is relatively longer, the carpus is flatter, the first metacarpal has stouter proportions, and the ungual on the third digit is particularly small (Fig. 2D and Table 1) (10). The pelvic girdle is similar in structure to that of *Allosaurus* (Fig. 2B). The ilium has a moderately developed supraacetabular crest and brevis fossa, the ischium has a trapezoidal obturator process and well-developed distal foot, and the pubis has a slender shaft and small distal foot. The hind limb has more elongate distal segments than in *Allosaurus* (Table 1). The femur is only slightly longer than the tibia and has a broad wing-shaped anterior trochanter. The astragalus preserves the base of a low plate-shaped ascending process (Fig. 2E), and the foot is slender and elongate (Fig. 2C).

Jurassic and Cretaceous theropods belong to one of two clades, Ceratosauria and Tetanurae (11), which diverged during the Late Triassic (Fig. 3). The skeletal remains of *Afrovenator* clearly indicate that it belongs within the tetanuran radiation (Fig. 3A) (12). Tetanuran synapomorphies in the skull include an opening in the antorbital fossa (maxillary fenestra), a pneumatic excavation in the jugal, and the position of the posteriormost maxillary tooth (anterior to the orbit) (Fig. 2A). Tetanuran synapomorphies in the postcranial skeleton include specialized wrist bones that constrain motion of the hand to a transverse plane (semilunate carpal with an articular troch-

Table 1. Length measurements (millimeters) and ratios in *Afrovenator* and *Allosaurus* (10). All unguals are measured perpendicular to the articular end. Parentheses indicate estimation.

Measurement	<i>Afrovenator</i>	<i>Allosaurus</i>
<i>Forelimb</i>		
Humerus (h)	(400)	310
Metacarpal I (I)	62	73
Metacarpal II (II)	135	123
Digit I—phalanx 1 (I-1)	112	136
Digit I, ungual	80	102
Digit II, ungual	76	92
Digit III—phalanx 3	53	53
Digit III, ungual	40	54
I/h	0.16	0.24
II/h	0.34	0.40
I/II	0.46	0.59
I/I-1	0.55	0.54
<i>Hind limb</i>		
Femur (f)	760	850
Tibia (t)	(687)	690
Metatarsal I (I)	103	85
Metatarsal IV (IV)	321	275
Digit II—phalanx 1	122	120
Digit II (or III) ungual	76	(72)
Digit IV—phalanx 1	90	75
Digit IV—phalanx 2	106	50
Digit IV—phalanx 3	87	30
t/f	0.90	0.81
IV/t	0.47	0.40
I/IV	0.32	0.31

P. C. Sereno, J. A. Wilson, H. C. E. Larsson, Department of Organismal Biology and Anatomy, University of Chicago, 1027 East 57 Street, Chicago, IL 60637, USA.
 D. B. Dutheil, 48 rue de la Rochefoucauld, 75009 Paris, France.
 H.-D. Sues, Department of Vertebrate Palaeontology, Royal Ontario Museum, 100 Queen's Park, Toronto, Ontario M5S 2C6, Canada.

*To whom correspondence should be addressed.